CME LIVE OPEN ACCESS

Journal of
Earth & Environmental Waste Management

Research Article ISSN: 3065-8799

Investigating the Co-loading of Doxorubicin and Melittin on Polyethylene Glycol at Different Molar Ratios Using Molecular Dynamics Simulation

Maryam Minaeian, Fatemeh Sadat Miraskarshahi and Azadeh Kordzadeh*

Chemical and Petroleum Engineering Department, Sharif University of Technology, Tehran, Iran.

Corresponding Author: Azadeh Kordzadeh, Chemical and Petroleum Engineering Department, Sharif University of Technology, Tehran, Iran.

Received: 2025 Jan 09 **Accepted:** 2025 Jan 28 **Published:** 2025 Feb 06

Abstract

The co-loading of melittin (MLT) and doxorubicin (DOX) on polyethylene glycol (PEG) at different molar ratios was investigated with molecular dynamics (MD) simulation. The interaction potential between drug molecules and PEG was evaluated with Lennard-Jones (LJ) and electrostatic potentials. Also, the conformational change was calculated to assess. The results indicated that the 1:2 (DOX: MLT) molar ratio has a strong binding energy with PEG, and also, at this molar ratio, the secondary structure of MLT is the same as that of the water medium. At a molar ratio of (2:1) (DOX: MLT), the secondary structure of the MLT and, as a result, its properties have changed, so this ratio is not suitable for co-loading of DOX and MLT on PEG. The obtained results at the molecular level are suitable for designing drug carriers based on drugs and polymers.

Keywords: Polyethylene Glycol, Melittin, Molecular Dynamics, Drug Delivery

1. Introduction

Cancer, responsible for one in six global deaths, stands as the second leading cause of mortality, trailing only cardiovascular diseases [1,2]. Patients were offered limited options, including single or combined treatments such as surgery, radiation therapy, and chemotherapy, albeit with constrained choices [3,4].

Nonetheless, the pursuit of novel cancer treatments remains a global challenge [5]. The quest for innovative therapies that precisely target tumor cells without affecting normal cells has driven extensive research in the past decades [6]. Aiming to enhance the cure and survival rates for cancer patients, the development and application of diverse drug delivery systems (DDSs) have emerged as promising avenues in cancer treatment. This dynamic approach seeks to revolutionize the landscape of cancer therapeutics [7]. DDSs can, in principle, provide enhanced efficacy and reduced toxicity for anticancer agents [8].

Therefore, developing DDSs is considered a great revolution in medical purposes to address specific challenges and provide more targeted and controlled delivery of therapeutic agents. Recent studies have shown that the combination of two drugs, dual-delivery, could improve the efficiency of drugs compared to conventional DDSs, which deliver a single drug for its intended therapeutic effect. Generally, dual-delivery is considered a high-efficiency system due to enhanced therapeutic efficacy, combinatorial treatment, reduced drug resistance, targeted delivery, and therapeutic flexibility [9,10].

Recent nanotechnology advancements have unveiled nanoparticles' remarkable potential as drug carriers. Due to their small size, these nanoparticles exhibit distinctive physicochemical and biological attributes that render them highly desirable for diverse biomedical applications. This promising avenue holds significant potential for reshaping therapeutic approaches [11]. Various classes of drug carrier nanoparticles have been investigated, including liposomes, carbon nanotubes (CNTs), and polymer-based carriers [12-18].

Polymer-based carriers have emerged as a strategic solution in drug delivery, adept at navigating complex physiological environments. Tailoring polymer molecular structures allows precise responses to external conditions guided by an in-depth understanding of underlying mechanisms. Integrating therapeutics with polymers introduces dynamism, enabling inherent therapeutic effects through bioactivity or optimizing release kinetics and curbing carrier accumulation via biodegradability [19]. N-(2-Hydroxypropyl) methacrylamide (HPMA) (polymer-drug), polyethylene glycol (PEG) (polymer-protein), (glutamic acid), dextran, dextrin, chitosans, poly (l-lysine), and poly (aspartamides) as potential polymeric carriers [20].

PEG represents a series of amphiphilic polymers 14 characterized by a common backbone of repeating ethylene glycol units [(⟦⟦CH⟧_2 ⟦CH⟧_2 O⟧_n)], differing primarily in molecular weights [21]. Among various polymers, PEG stands out for its significant biomedical applications, attributable to its non-toxicity, non-immunogenicity, excellent biocompatibility, and resistance to protein adsorption [22,23]. In DDSs, PEG molecules contribute by shielding both the DDSs and the encapsulated drugs with their extended hydrophilic chains [24]. Moreover, PEG's terminal hydroxyl group renders it versatile as a carrier material, allowing for conjugation with numerous active drug molecules to create effective drug delivery systems [25].

One of the most studied DDSs is peptide-based DDSs, which have many advantages compared to synthetic systems. As a short chain of amino acids linked by chemical bonds, peptides have an essential and structural role in constructing smart DDSs; in addition to having the mentioned goals, peptides have better biochemical and biophysical attributes, precise control of molecular weight through solid-phase synthesis and purification, cost-effectiveness, adjustable bioactivity, and a diverse chemical range. Hence, peptides have the potential to be utilized as a delivery system of anticancer drugs and/or contrast agents for visualizing tumor-related abnormalities [26-28]. Melittin (MLT), a fundamental polypeptide composed of 26 amino acids, accounts for nearly half of the dry weight of honeybee venom [29]. This peptide lacks a disulfide bridge, featuring a predominantly hydrophobic N-terminal region and a C-terminal section that is both hydrophilic and potently basic. In aqueous solutions, melittin aggregates into tetramers, but it also has the innate ability to assimilate into cell membranes. Considering the hemolytic properties of melittin and to prevent its degradation, it is necessary to use a carrier for melittin [30].

Doxorubicin (DOX) belongs to the anthracycline category of chemotherapy drugs. Its main mode of action centers on its capacity to insert itself between DNA base pairs, leading to DNA strand disruption and hindering both DNA and RNA synthesis. Furthermore, by inhibiting the enzyme topo isomerase 2, doxorubicin decelerates or halts cancer cell proliferation, as this enzyme is vital for the division and growth of these cells [31].

It is indicated that the co-loading of paclitaxel and MLT on lipodisk with a diameter of 50 nm successfully affects the treatment of glioma [32]. Hematyar et al. demonstrated that citric acid-functionalized Fe3O4 magnetic nanoparticles loaded with DOX and MLT have anti-tumor activity [33]. Also, this co-loading of DOX and MLT is due to electrostatic interactions. It clarified that the co-delivery of MLT and curcumin from chitosan functionalized α-lactalbumin nanotubes could induce cancer cell apoptosis [34]. Li et al. synthesized a pH-sensitive polymersome for the co-delivery of DOX that could solve the multi-drug resistance problem [35,36].The peptide conformation determines its properties. One of the critical factors is that the carrier used does not change the conformation of the peptide, which cannot be evaluated in laboratory and macroscopic methods and requires precise molecular techniques such as molecular dynamic simulation to investigate atomic interactions.

Our investigations have revealed that the precise mechanism governing the interaction between the drug and the polymer remains ambiguous in laboratory experiments. The molecular dynamics simulation was performed to elucidate this interaction and discern the intricacies of the drug-polymer interplay. Our study demonstrates the compatibility, properties, and structure of Melittin when combined with anticancer agents like Doxorubicin, underscoring the significance of PEG as the carrier in drug delivery systems [37-40]. In this study, the co-loading of DOX and MLT at different molar ratios on PEG chains was simulated. The interaction potentials between DOX and MLT with PEG were calculated. Also, the conformational changes of the MLT were evaluated to select an optimum molar ratio for the co-loading of DOX and MLT on PEG chains.

2. Materials and Method

2.1. The Structural Model

The MLT structure was obtained from the protein data bank (PDBID=6DST). The pdb file of DOX obtained from the DRUGBANK server [41,42]. A PEG chain with 25 monomer was built with CHARMM-GUI server [43].

2.2. Force Field

For all simulations, the GROMACS 5.1.4 simulation package was utilized [44]. Molecular visualization was facilitated by the visual molecular dynamics (VMD 1.9.1) program [45].

The GROMOS54A7 force field was employed for accurate calculations of both bonded and nonbonded interactions [46]. Water molecules were represented using the simple point charge model [47].

2.3. MD Simulation

This study conducted a series of simulations at three molar ratios of DOX to MLT, which are 1:2, 2:1, and 1:1. In each simulation box, 5 PEG chains were used as polymer-carriers. The size of the simulation box is 10 ×10 ×10 nm3 for all simulations. The concentrations were selected based on experimental studies [48]. These simulations were meticulously executed within a consistent and controlled environment to ensure the robustness of the findings. Also, the melittin was simulated in a water medium without DOX and PEG as a reference system to evaluate its conformational changes after loading on PEG.

The NPT ensemble was used to delve into the specifics. Throughout the entire simulation period, which spanned a considerable duration, the simulation box temperature was 310 K, representing physiological conditions. This temperature control was achieved using a Nose'-Hoover thermostat [49]. Simultaneously, the pressure held at a constant 1 bar, expertly regulated through the employment of the Parrinello–Rahman barostat, which harnessed semi-isotropic pressure coupling [50].

The simulation was meticulously chosen to ensure precision in modeling dynamic interactions within the system [51]. To guarantee the integrity of the molecular structure, the Linear Constraint Solver (LINCS algorithm) was applied to preserve bond constraints throughout the simulation meticulously. Long-range electrostatic forces were meticulously calculated using the highly effective particle mesh Ewald method in intermolecular interactions. A cutoff radius of 1.2 nm was judiciously selected for this calculation to optimize computational efficiency. The Lennard-Jones (LJ) and coulombic potential models were used for calculation of van der Waals (vdW) and electrostatic interactions.

The simulation protocol commenced with an NVT simulation, lasting 10 ns, rigorously aligned with the physiological temperature of 310 K. Subsequently, it transitioned into an NPT ensemble simulation, maintaining the pressure at 1 bar, and continued for an additional 20 ns. Finally, it embarked on a comprehensive 100 ns molecular dynamics (MD) step, meticulously collecting data for our analyses. It is worth noting that the last 30 ns of this simulation period were dedicated to the detailed analysis of the acquired data, allowing for comprehensive insights into the intricacies of the systems under investigation.

3. Results and Discussion

3.1. Interaction Potential

Figure 1 displays the snapshots of the co-loading of DOX and MLT on PEG chains at three molar ratios. Initially, within each molar ratio, Doxorubicin and Melittin are evenly dispersed around the PEG chains in the simulation box. Co-loading on PEG, facilitated by vdW and electrostatic interactions, becomes evident as the simulation progresses. These interactions are quantified using the Lennard-Jones (LJ) model for instantaneous polarities and the Coulombic model for charged or partially charged atoms. Figures 2, 3, and 4 illustrate the LJ and electrostatic potentials during the co-loading of DOX and MLT on PEG at (1:1), (1:2), and (2:1) molar ratios, respectively. Negative LJ potential values indicate the attraction between molecules. Table 1 presents the average LJ and electrostatic potential values. The results in Table 1 revealed that the DOX and MLT at a molar ratio 1:2 had the strongest binding energy to PEG. The low fluctuations of potentials explained the simulated system's equilibration and the simulation time's sufficiency. These results are in accordance with previous studies [52,53].

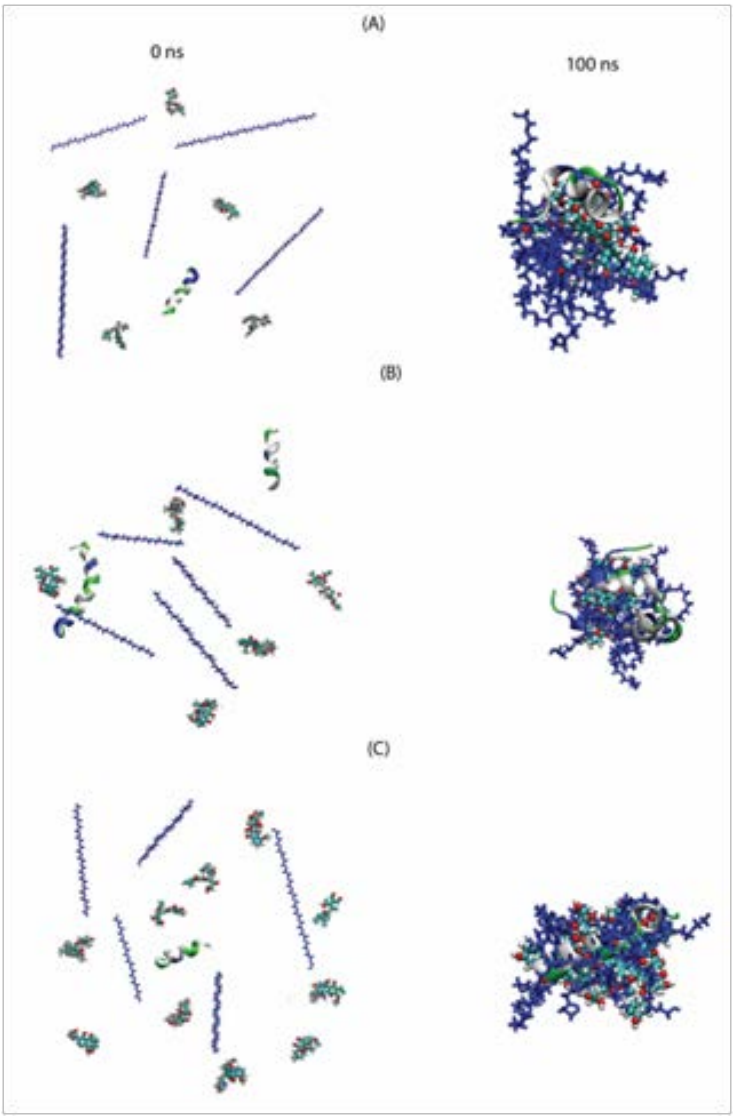

Figure 1: The Snapshots of MLT and DOX Co-Loading on PEG Chains at (A) 1:1, (B) 1:2, and (C) 2:1 Molar Ratio

The PEG chains are shown with blue color. The carbon, nitrogen, hydrogen and oxygen atoms in DOX are shown with cyan, blue, white and red colors, respectively. The nonpolar, polar and basic amino acids of MLT are show with white, green, and blue colors, respectively. The water molecules were ignored for clarity.

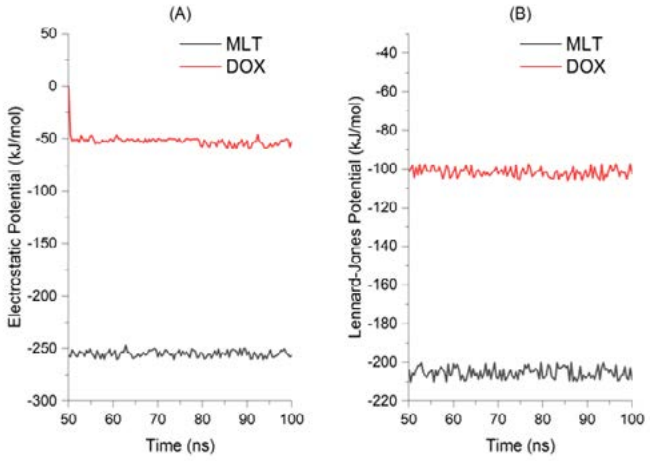

Figure 2: (A) Electrostatic and (B) Lennard Jones (LJ) Potentials of MLT and DOX with PEG at Molar Ratio of 1:1 (DOX: MLT)

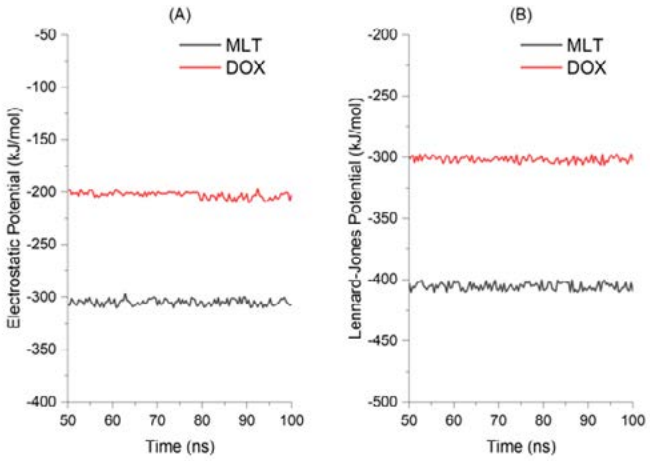

Figure 3: (A) Electrostatic and (B) Lennard Jones (LJ) Potential of MLT and DOX with PEG at Molar Ratio of 1:2 (DOX: MLT)

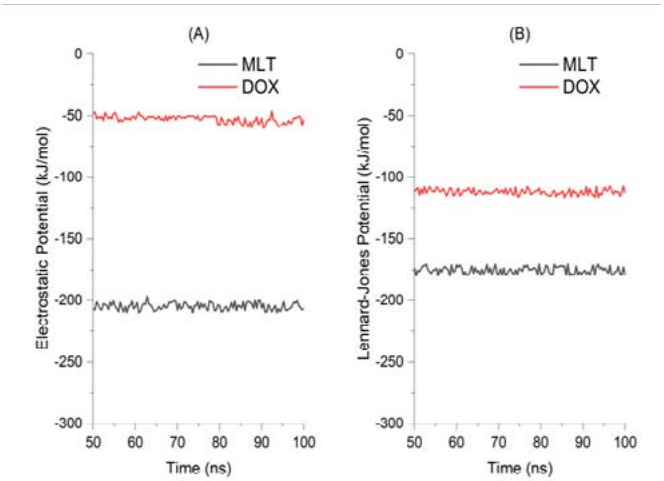

Figure 4: (A) Electrostatic and (B) Lennard Jones (LJ) Potential of MLT and DOX with PEG at Molar Ratio of 2:1 (DOX: MLT)

	DOX			MLT		
	LJ	ELE	BE	LJ	ELE	BE
1:1	-102	-55	-157	-203	-251	-454
1:2	-305	-210	-515	-402	-303	-705
2:1	-110	-49	-159	-185	-212	-397

Table 1: The Averaged Values of LJ and Electrostatic Potentials (kJ/mol) between DOX and MLT and PEG Chains

3.2. Radial Distribution Function

To evaluate the adsorption of DOX and MLT on PEG chains, the radial distribution function (RDF) was calculated, illustrated in Figure 5. The RDF is the probability of finding one molecule around another. In Figure 5 (A), for the 1:1 (DOX: MLT) molar ratio, the higher RDF peak of melittin than DOX suggests a greater probability of finding melittin near PEG. This is in accordance with Table 1, which indicates melittin has stronger binding energy with PEG. The RDF plot of DOX and MLT at a molar ratio of 1:2 in Figure 5 (B) exhibits RDF peaks for both doxorubicin and melittin, which are nearly equal in height. This similarity suggests a comparable probability of finding DOX and MLT around PEG, a finding further supported by the similar binding energies of DOX and MLT with PEG listed in Table 1. Lastly, Figure 5 (C) reveals that the RDF peak for doxorubicin is lower than melittin at a molar ratio of 2:1 (DOX: MLT). These results are in accordance with previous studies [54,55].

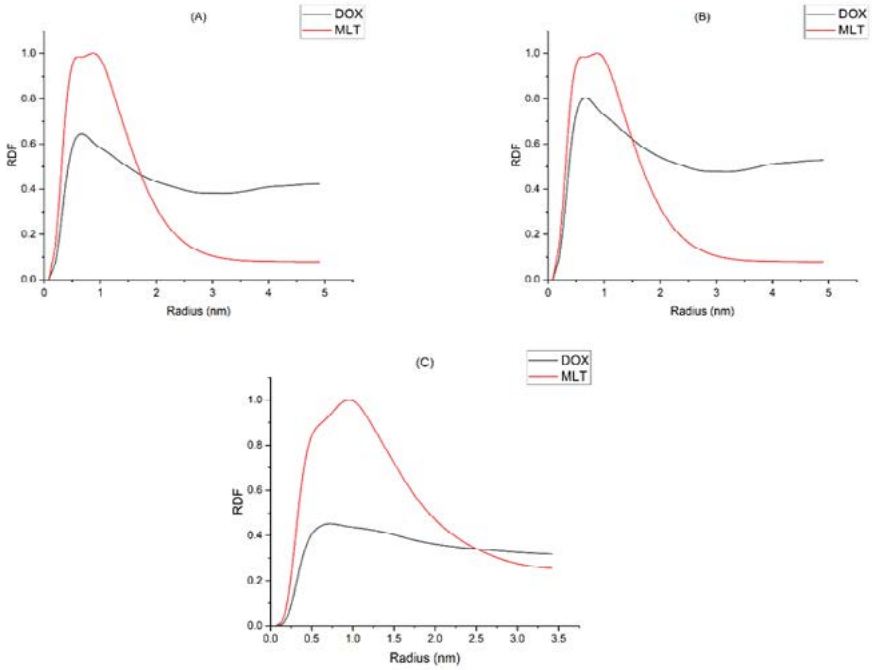

Figure 5: The RDF Plot of MLT and DOX Around PEG at Molar Ratios of (A) 1:1, (B) 1:2, and (C) 2:1 (DOX:MLT)

3.3. Conformational Changes of Melittin

As it is illustrated in Figure 6 (A), the radius of gyration of melittin in water medium equals 1.021 nm. The radius of gyration of melittin after adsorption on PEG chains at molar ratios of (1:1) and (1:2) (DOX:MLT) are similar to water medium. While, the radius of gyration of melittin reached to 3.621 nm after adsorption on PEG chains at molar ratio of (2:1) (DOX:MLT). From these observations, it can be inferred that the radius of gyration of melittin increases with a higher concentration of doxorubicin. This suggests that the melittin structure becomes more disturbed as the amount of doxorubicin increases, providing additional evidence to support this claim.

The root mean square fluctuations (RMSF) analysis was performed to evaluate the structural changes of melittin after adsorption on PEG chins. The obtained results in Figure 6 (B) elucidated that the residual fluctuations of melittin in water medium and after adsorption on PEG at molar rations of (1:1) and (1:2) are similar. At the same time, the residual fluctuations of melittin after adsorption on PEG at a molar ratio of (2:1) are different from the water medium, confirming the structural changes of melittin at a high concentration of DOX. These results are in accordance with previous studies [56,57].

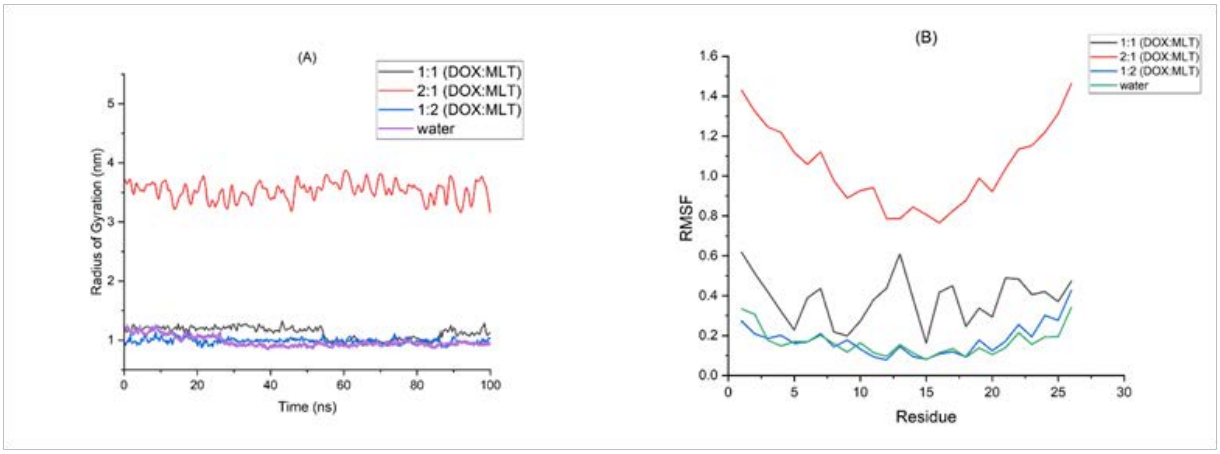

Figure 6: (A) The Radius of Gyration, and (B) RMSF of MLT in Water Solution and After Adsorption on PEG at Different Molar Ratios

3.4. Secondary Structure of Melittin

This section evaluated the secondary structure of melittin in a water medium and after the adsorption of PEG at different molar ratios. This approach helps identify an optimal carrier that preserves melittin's properties in an aquatic environment. The results in Figure 7 demonstrated that melittin in a water medium has mainly an alpha helix structure. The coil and 5-helix structure were observed in melittin after adsorption on PEG at molar ratios of (1:1) and (2:1) (DOX: MLT). The secondary structure of melittin after adsorption on PEG at a molar ratio of (1:2) (DOX: MLT) is similar to that of a water medium. Therefore, this ratio has a more favorable adaptation of melittin's structure, potentially aiding in maintaining its effectiveness. These results are in accordance with previous studies [56,57].

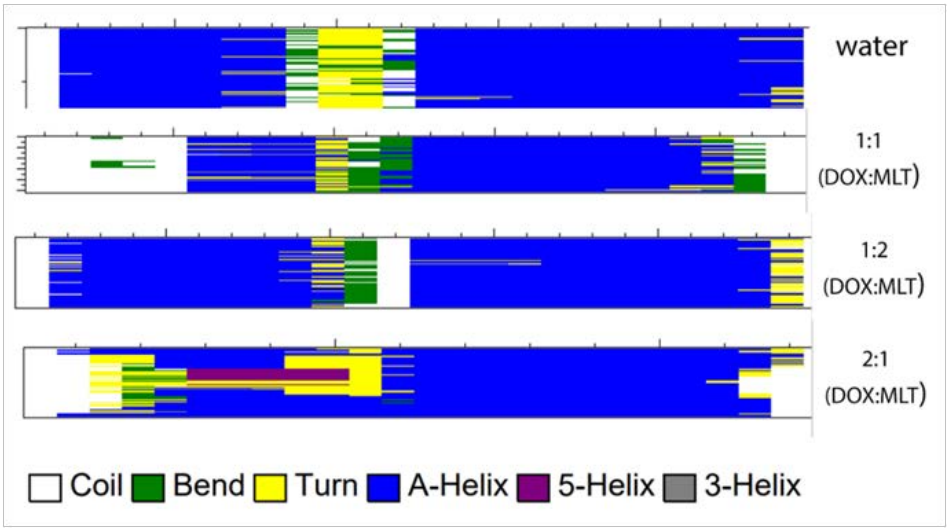

Figure 7: The Secondary Structure of MLT in Water Solution and After Adsorption on PEG at Different Molar Ratios

4. Conclusion

In this study, the co-loading of doxorubicin (DOX) and melittin (MLT) on polyethylene glycol (PEG) was investigated using molecular dynamics (MD) simulation. The interaction potentials and radial distribution function (RDF) were analyzed. The results showed that DOX and MLT at a molar ratio of (1:2) have the strongest binding energy with PEG. Also, in addition to the potential for interaction, the conformational changes of MLT are important for selecting suitable conditions. The results demonstrated that the radius of gyration of melittin has increased to 3.621 nm after adsorption on PEG at a molar ratio of (2:1), and also, the 5-helix alpha D structure has appeared on its secondary structure. Therefore, the molar ratio of (2:1) (DOX: MLT) has changed the structure and properties of melittin. Meanwhile, at a ratio of 1:2, the properties of MLT are the same as those of water medium. These results obtained at the molecular scale help design dual drug delivery systems.

References

1. Debela, D. T., Muzazu, S. G., Heraro, K. D., Ndalama, M. T., Mesele, B. W., Haile, D. C., ... & Manyazewal, T. (2021). New approaches and procedures for cancer treatment: Current perspectives. *SAGE open medicine, 9*, 20503121211034366.
2. Nair, A. R., & Mon, R. S. RESEMBLANCE AND UNDERSTANDING OF CANCER TREATMENT USING CANCER NANO MEDICINE AND HOMOEOPATHY.
3. Knight, S. R., Shaw, C. A., Pius, R., Drake, T. M., Norman, L., Ademuyiwa, A. O., ... & Fermani, C. G. (2021). Global

variation in postoperative mortality and complications after cancer surgery: a multicentre, prospective cohort study in 82 countries. *The Lancet, 397*(10272), 387-397.
4. Roy, A., & Li, S. D. (2016). Modifying the tumor microenvironment using nanoparticle therapeutics. *Wiley Interdisciplinary Reviews: nanomedicine and nanobiotechnology, 8*(6), 891-908.
5. Siegel, R. L., Miller, K. D., Fuchs, H. E., & Jemal, A. (2021). *Cancer statistics, 2021. CA: a cancer journal for clinicians, 71*(1), 7-33.
6. Yao, Y., Zhou, Y., Liu, L., Xu, Y., Chen, Q., Wang, Y., ... & Shao, A. (2020). Nanoparticle-based drug delivery in cancer therapy and its role in overcoming drug resistance. *Frontiers in molecular biosciences, 7,* 193.
7. Liu, G., Yang, L., Chen, G., Xu, F., Yang, F., Yu, H., ... & Li, B. (2021). A review on drug delivery system for tumor therapy. *Frontiers in Pharmacology, 12*, 735446.
8. Thacharodi, D., & Rao, K. P. (1995). Development and in vitro evaluation of chitosan-based transdermal drug delivery systems for the controlled delivery of propranolol hydrochloride. *Biomaterials, 16*(2), 145-148.
9. Berillo, D., Yeskendir, A., Zharkinbekov, Z., Raziyeva, K., & Saparov, A. (2021). Peptide-based drug delivery systems. *Medicina, 57*(11), 1209.
10. Wei, L., Cai, C., Lin, J., & Chen, T. (2009). Dual-drug delivery system based on hydrogel/micelle composites. *Biomaterials, 30*(13), 2606-2613.
11. Wilczewska, A. Z., Niemirowicz, K., Markiewicz, K. H., & Car, H. (2012). Nanoparticles as drug delivery systems. *Pharmacological reports, 64*(5), 1020-1037.
12. Samad, A., Sultana, Y., & Aqil, M. (2007). Liposomal drug delivery systems: an update review. *Current drug delivery, 4*(4), 297-305.
13. Allen, T. M., & Cullis, P. R. (2013). Liposomal drug delivery systems: from concept to clinical applications. *Advanced drug delivery reviews, 65*(1), 36-48.
14. Kordzadeh, A., Amjad-Iranagh, S., Zarif, M., & Modarress, H. (2019). Adsorption and encapsulation of the drug doxorubicin on covalent functionalized carbon nanotubes: A scrutinized study by using molecular dynamics simulation and quantum mechanics calculation. *Journal of Molecular Graphics and Modelling, 88,* 11-22.
15. Kordzadeh, A., Zarif, M., & Amjad-Iranagh, S. (2023). Molecular dynamics insight of interaction between the functionalized-carbon nanotube and cancerous cell membrane in doxorubicin delivery. *Computer Methods and Programs in Biomedicine, 230,* 107332.
16. Kordzadeh, A., Sa, A. R., & Mashayekhan, S. (2023). Adsorption and encapsulation of melittin on covalently functionalized carbon nanotubes; a molecular dynamics simulation study. *Computers in Biology and Medicine, 166*, 107393.
17. Guo, X., Wang, L., Wei, X., & Zhou, S. (2016). Polymer-based drug delivery systems for cancer treatment. *Journal of Polymer Science Part A: Polymer Chemistry, 54*(22), 3525-3550.
18. Tong, X., Pan, W., Su, T., Zhang, M., Dong, W., & Qi, X. (2020). Recent advances in natural polymer-based drug delivery systems. *Reactive and Functional Polymers, 148*, 104501.
19. Liechty, W. B., Kryscio, D. R., Slaughter, B. V., & Peppas, N. A. (2010). Polymers for drug delivery systems. *Annual review of chemical and biomolecular engineering, 1*(1), 149-173.
20. Vilar, G., Tulla-Puche, J., & Albericio, F. (2012). Polymers and drug delivery systems. *Current drug delivery, 9*(4), 367-394.
21. Mishra, P., Nayak, B., & Dey, R. K. (2016). PEGylation in anti-cancer therapy: An overview. *Asian journal of pharmaceutical sciences, 11*(3), 337-348.
22. Liu, S., Li, K., Hussain, I., Oderinde, O., Yao, F., Zhang, J., & Fu, G. (2018). A Conductive Self-Healing Double Network Hydrogel with Toughness and Force Sensitivity. *Chemistry–A European Journal, 24*(25), 6632-6638.
23. Geng, Y., Duan, H., Xu, L., Witman, N., Yan, B., Yu, Z., ... & Fu, W. (2021). BMP-2 and VEGF-A modRNAs in collagen scaffold synergistically drive bone repair through osteogenic and angiogenic pathways. *Communications Biology, 4*(1), 82.
24. Kim, A., Yun, M. O., Oh, Y. K., Ahn, W. S., & Kim, C. K. (1999). Pharmacodynamics of insulin in polyethylene glycol-coated liposomes. *International journal of pharmaceutics, 180*(1), 75-81.
25. Wang, Y., Zhang, S., & Benoit, D. S. (2018). Degradable poly (ethylene glycol)(PEG)-based hydrogels for spatiotemporal control of siRNA/nanoparticle delivery. *Journal of Controlled Release, 287*, 58-66.
26. Gupta, V., Bhavanasi, S., Quadir, M., Singh, K., Ghosh, G., Vasamreddy, K., ... & Banerjee, S. K. (2019). Protein PEGylation for cancer therapy: bench to bedside. *Journal of Cell Communication and Signaling, 13*, 319-330.
27. Tesauro, D., Accardo, A., Diaferia, C., Milano, V., Guillon, J., Ronga, L., & Rossi, F. (2019). Peptide-based drug-delivery systems in biotechnological applications: recent advances and perspectives. *Molecules, 24*(2), 351.
28. Lian, Z., & Ji, T. (2020). Functional peptide-based drug delivery systems. *Journal of Materials Chemistry B, 8*(31), 6517-6529.
29. Chen, J., Guan, S. M., Sun, W., & Fu, H. (2016). Melittin, the major pain-producing substance of bee venom. *Neuroscience bulletin, 32*, 265-272.
30. Terwilliger, T. C., & Eisenberg, D. (1982). The structure of melittin. II. *Interpretation of the structure.*
31. Sritharan, S., & Sivalingam, N. (2021). A comprehensive review on time-tested anticancer drug doxorubicin. *Life sciences, 278*, 119527.
32. Wang, H., Wang, S., Wang, R., Wang, X., Jiang, K., Xie, C., ... & Lu, W. (2019). Co-delivery of paclitaxel and melittin by glycopeptide-modified lipodisks for synergistic anti-glioma therapy. *Nanoscale, 11*(27), 13069-13077.
33. Hematyar, M., Soleimani, M., Es-Haghi, A., & Rezaei Mokarram, A. (2018). Synergistic co-delivery of doxorubicin and melittin using functionalized magnetic nanoparticles for cancer treatment: loading and in vitro release study by LC–MS/MS. *Artificial cells, nanomedicine, and biotechnology, 46*(sup3), 1226-1235.
34. Hou, G., Li, Y., Wang, Q., Zhang, H., Liang, S., Liu, B., & Shi, W. (2022). iRGD-grafted N-trimethyl chitosan-coated

protein nanotubes enhanced the anticancer efficacy of curcumin and melittin. *International Journal of Biological Macromolecules, 222,* 348-359.

35. Li, N., Zhang, P., Huang, C., Song, Y., Garg, S., & Luan, Y. (2015). Co-delivery of doxorubicin hydrochloride and verapamil hydrochloride by pH-sensitive polymersomes for the reversal of multidrug resistance. *RSC advances, 5*(95), 77986-77995.
36. Han, E., Kim, D., Cho, Y., Lee, S., Kim, J., & Kim, H. (2023). Development of polymersomes co-delivering doxorubicin and melittin to overcome multidrug resistance. *Molecules, 28*(3), 1087.
37. Sun, S., Cui, Y., Yuan, B., Dou, M., Wang, G., Xu, H., ... & Peng, C. (2023). Drug delivery systems based on polyethylene glycol hydrogels for enhanced bone regeneration. *Frontiers in bioengineering and biotechnology, 11,* 1117647.
38. Burley, S. K., Berman, H. M., Bhikadiya, C., Bi, C., Chen, L., Di Costanzo, L., ... & Zardecki, C. (2019). RCSB Protein Data Bank: biological macromolecular structures enabling research and education in fundamental biology, biomedicine, biotechnology and energy. *Nucleic acids research, 47*(D1), D464-D474.
39. Kolate, A., Baradia, D., Patil, S., Vhora, I., Kore, G., & Misra, A. (2014). PEG—A versatile conjugating ligand for drugs and drug delivery systems. *Journal of controlled release, 192,* 67-81.
40. Wang, A., Zheng, Y., Zhu, W., Yang, L., Yang, Y., & Peng, J. (2022). Melittin-based nano-delivery systems for cancer therapy. *Biomolecules, 12*(1), 118.
41. Bank, P. D. (1971). Protein data bank. *Nature New Biol, 233*(223), 10-1038.
42. Wishart, D. S., Feunang, Y. D., Guo, A. C., Lo, E. J., Marcu, A., Grant, J. R., ... & Wilson, M. (2018). DrugBank 5.0: a major update to the DrugBank database for 2018. *Nucleic acids research, 46*(D1), D1074-D1082.
43. Jo, S., Kim, T., Iyer, V. G., & Im, W. (2008). CHARMM-GUI: a web-based graphical user interface for CHARMM. *Journal of computational chemistry, 29*(11), 1859-1865.
44. Van Der Spoel, D., Lindahl, E., Hess, B., Groenhof, G., Mark, A. E., & Berendsen, H. J. (2005). GROMACS: fast, flexible, and free. *Journal of computational chemistry, 26*(16), 1701-1718.
45. Humphrey, W., Dalke, A., & Schulten, K. (1996). VMD: visual molecular dynamics. *Journal of molecular graphics, 14*(1), 33-38.
46. Schmid, N., Eichenberger, A. P., Choutko, A., Riniker, S., Winger, M., Mark, A. E., & Van Gunsteren, W. F. (2011). Definition and testing of the GROMOS force-field versions 54A7 and 54B7. *European biophysics journal, 40*, 843-856.
47. Berendsen, H. J., Postma, J. P., van Gunsteren, W. F., & Hermans, J. (1981). Interaction models for water in relation to protein hydration. In Intermolecular forces: proceedings of the fourteenth Jerusalem symposium on quantum chemistry and biochemistry held in jerusalem, israel, april 13–16, 1981 (pp. 331-342). *Springer Netherlands.*
48. Liu, Z., Sun, X., Nakayama-Ratchford, N., & Dai, H. (2007). Supramolecular chemistry on water-soluble carbon nanotubes for drug loading and delivery. *ACS nano, 1*(1), 50-56.
49. Evans, D. J., & Holian, B. L. (1985). The nose–hoover thermostat. *The Journal of chemical physics, 83*(8), 4069-4074.
50. Saito, H., Nagao, H., Nishikawa, K., & Kinugawa, K. (2003). Molecular collective dynamics in solid para-hydrogen and ortho-deuterium: The Parrinello–Rahman-type path integral centroid molecular dynamics approach. *The Journal of chemical physics, 119*(2), 953-963.
51. Hess, B., Bekker, H., Berendsen, H. J., & Fraaije, J. G. (1997). LINCS: a linear constraint solver for molecular simulations. *Journal of computational chemistry, 18*(12), 1463-1472.
52. de Almeida, A. R., Colherinhas, G., & de Andrade, D. X. (2023). Effects of Coulomb and vdW modifiers on hydrogen-bonds, energy and structural properties of peptide nanomembranes: A study by Molecular Dynamics simulations. *Journal of Molecular Liquids, 382,* 122017.
53. Mendanha, K., Oliveira, L. B. A., & Colherinhas, G. (2022). Modeling, energetic and structural analysis of peptide membranes formed by arginine and phenylalanine (R2F4R2) using fully atomistic molecular dynamics. *Journal of Molecular Liquids, 367*, 120498.
54. de Sousa, E. R., de Andrade, D. X., & Colherinhas, G. (2022). EF4K bola-amphiphilic peptide nanomembrane: structural, energetic and dynamic properties using molecular dynamics. *Journal of Molecular Liquids, 368,* 120651.
55. Fehér, B., Gascoigne, L., Giezen, S. N., & Voets, I. K. (2022). Impact of arginine modified SNARE peptides on interactions with phospholipid bilayers and coiled-coil formation: A molecular dynamics study. *Journal of Molecular Liquids, 364*, 119972.
56. Wu, X., Huan, X., Zhu, Y., Yang, G., Yang, H., Wu, Z., & Xu, W. (2023). Co-loading of doxorubicin and anti-cancer peptide LL-37 on covalently functionalized carbon nanotubes; a molecular dynamics simulation study. *Journal of Molecular Liquids, 386*, 122444.
57. Alves, E. D., de Andrade, D. X., de Almeida, A. R., & Colherinhas, G. (2022). Molecular dynamics study of hydrogen bond in peptide membrane at 150–300 K. *Journal of Molecular Liquids, 349*, 118165.